ISSN 0974 - 9373

Vol. 22 No. 2 (2018) **Journal of International Academy of Physical Sciences** pp. 85- 111

Quasi-Static Deformation Caused by Seismic and Heat Sources in a Thermoelastic Solid in Contact with a Porous Solid

Anil K. Vashishth

Department of Mathematics
Kurukshetra University, Kurukshetra 136119, India
Email: akvashishth@kuk.ac.in

Kavita Rani

Department of Mathematics
C.M.G. Govt. College for Women, Bhodia Khera, Fatehabad 125050, India
Email: karya4@gmail.com

(Received February 06, 2018)

Abstract: A study of deformation, with quasi-static assumption, of a medium, which consists of thermoelastic solid and poroelastic solid half-spaces, due to seismic sources and heat source in thermoelastic solid is carried out. The formulated quasi-static problem is solved using Airy's stress function approach. The expressions of Airy's stress function and temperature difference function in an unbounded thermoelastic medium due to various types of seismic sources and heat source are obtained. For line forces, dip-slip dislocation and line heat source in the thermoelastic solid medium, the solutions in the form of displacements, stresses, pore pressure and temperature difference function are obtained. For a vertical dip-slip dislocation, analytical solutions are derived for particular cases of adiabatic and isothermal conditions in the thermoelastic medium and undrained and drained conditions in the poroelastic medium. The results, so obtained, have been verified by making comparison with earlier results. Numerical results for displacements, pore pressure, temperature difference function and stresses have also been computed for vertical dip-slip fault. Temperature profile and stresses contours have also been plotted for line heat source.

Keywords: seismic sources, thermoelastic, poroelastic, dip-slip dislocation, heat source.

2010 AMS Classification Number: 74F05, 74F10, 74L05, 35Q74, 35E20, 35B30.

1. Introduction

The study of static response produced by seismic and/or heat source in a medium is significant in the fields like geomechanics, soil mechanics, hydrology, earthquake and structural engineering etc. To investigate the effect of a structural discontinuity on the deformation of a medium, it is appropriate to formulate a problem of a long fault in a model composed of two homogeneous half-spaces in welded contact and to find the analytical solution thereof. To explore the deformation caused by seismic sources, the two welded half-space models have been studied by many investigators[1-16].

The theory of poroelasticity deals with the mechanics of an elastic porous medium filled (thoroughly or partially) with pore fluid. It studies the coupling of the deformation of the rock/soil and flow of fluid in it. The Crust of the Earth can be treated as porous up to some extent. The interaction of solid skeleton and pore-fluid in saturated rocks/soil has drawn the attention of researchers. The linearized constitutive relations and governing equations for poroelastic medium were developed by Biot[17-18] and have been used by many investigators (Wang[19] and the references therein). The elastic constants, introduced by Biot, were replaced by Rice and Cleary[20] with Poisson ratio and bulk modulus evaluated in both the drained (constant pore pressure) and undrained (no flow) limits of long and short time behaviour, respectively. This formulation has also been adopted for many geophysical problems[21]. Rudnicki[22] derived fundamental solutions for point and line sources in an isotropic poroelastic medium. Pan[23] presented fundamental solutions of fluid and solid point dislocations in an infinite poroelastic medium. Taguchi and Kurashige[24] obtained fundamental solutions for point force and an instantaneous fluid point source in transversely isotropic poroelastic medium. Rani and Singh[25] investigated the quasi-static response of a poroelastic medium subjected to seismic sources in the connected elastic medium. Kumar et al.[26] considered a long tensile fault in an elastic half-space and computed the deformation caused by it in a poroelastic half-space. Kumar et al.[27] formulated a problem of a single force of acting in a poroelastic medium and obtained the closed-form analytical solutions. Kumari and Miglani[28-29] studied the plane strain problem of deformation induced by inclined line loads in isotropic and transversely isotropic elastic half-spaces in welded contact with a poroelastic half-space. Miglani and Kumari[30] discussed plain strain deformation, caused by inclined line loads, in two welded poroelastic half-spaces. Verma et al.[31] formulated a model of poroelastic layer lying over an elastic half-space and studied the deformation produced by a dip-slip fault in the elastic medium. Pan et al.[32] obtained two dimensional general solutions and fundamental solution for fluid-saturated, orthotropic, poroelastic materials.

A part of the interior of the Earth can be considered as thermoelastic due to strong dependence of properties on the temperature in the Mantle and the Core. Many deep seismic faults do occur in the lower Crust or upper Mantle layer of the Earth. So, for a realistic model, it is apt to represent the medium as a two-phase continuum, consisting of a poroelastic solid and a thermoelastic solid. A lot of literatures can be found on the problems of deformation due to seismic sources in elastic solids while that on poroelastic and thermoelastic solids is not so. Consideration of the fact, that some of the faults are very long, makes the two-dimensional fault model as adequate for many situations.

In this paper, quasi static plane problem of deformation of a medium, which consists of thermoelastic and poroelastic solids, is undertaken. This deformation and change in temperature is considered due to seismic and thermal sources. The expressions of temperature difference function and Airy stress function in a thermoelastic solid due to various types of sources, derived by Vashishth and Rani[33], are used. The general solutions for pore pressure, temperature difference function, stresses and displacements in both half-spaces have been derived. The case of vertical dip-slip fault is studied in detail and closed form solutions are obtained for two limits of long and short time: adiabatic and isothermal conditions in thermoelastic medium; undrained and drained conditions in poroelastic medium. The solutions in space-time domain are computed numerically. The results, obtained by Singh et al.[3], Rani and Singh[25] and Vashishth and Rani[33], are obtained as particular cases. It is observed that there is a significant temperature change due to seismic source in thermoelastic medium. The displacements in poroelastic medium are also influenced when the other half space is taken thermoelastic instead of elastic one.

2. Formulation of the Problem

A model consisting of a homogeneous isotropic poroelastic half-space $(z \leq 0)$ in welded contact with a homogeneous isotropic thermoelastic half-space $(z \geq 0)$, is considered. The interface $z = 0$ is adiabatic and impermeable. A line source (seismic or heat source), acting through the point $(0,0,h)$ and parallel to the x-axis, in the thermoelastic half space is considered (Fig. 1).

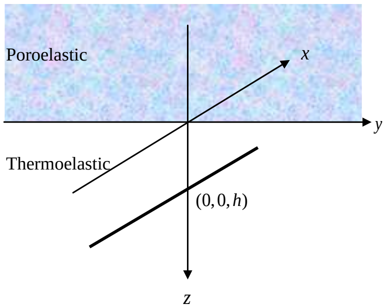

Figure 1. A line source acting through the point $(0,0,h)$ in thermoelastic half-space in welded contact to a poroelastic half-space

The displacement components, for a plane strain problem in yz-plane, are taken as

(2.1) $$u_i = u_i(y,z,t),\ u_i' = u_i'(y,z,t), \quad u_x = u_x' = 0, \quad (i = y, z)$$

where u_i and u_i' are displacement components in thermoelastic and poroelastic half-spaces respectively.

A thermoelastic medium is characterized by the parameters: λ, μ (Lame's constants), α_t (coefficient of linear thermal expansion), υ (Poisson's ratio), λ_0 (thermal conductivity), C_e (specific heat), ρ (density) and T_0 (reference temperature).

Following Vashishth and Rani[33], the Airy's Stress function $\bar{U}_0$ and temperature difference function $\bar{\theta}_0$ (in Laplace transform domain), for a line source acting through the point $(0,0,h)$ and parallel to the x-axis in an unbounded thermoelastic medium, can be represented as

(2.2) $$\bar{U}_0 = \int_0^\infty \Phi_0 \begin{pmatrix} \sin ky \\ \cos ky \end{pmatrix} dk,$$

(2.3) $$\bar{\theta}_0 = \int_0^\infty \Psi_0 \begin{pmatrix} \sin ky \\ \cos ky \end{pmatrix} dk,$$

where

(2.4) $$\Phi_0 = A_0^{\pm} e^{-m|z-h|} + (B_0^{\pm} + k|z-h| C_0^{\pm}) e^{-k|z-h|},$$

(2.5) $$\Psi_0 = \frac{s}{\gamma c} \zeta A_0^{\pm} e^{-m|z-h|} + k^2 \zeta C_0^{\pm} e^{-k|z-h|},$$

$$m = \left(k^2 + \frac{s}{c}\right)^{1/2}, \gamma = \frac{2(\upsilon - \upsilon_s)}{(1-\upsilon)}, c = \frac{\lambda_0 (\lambda + 2\mu)}{\rho C_e (\lambda_s + 2\mu)}, \zeta = \frac{2(\upsilon_s - \upsilon)}{\alpha_0},$$

$$\alpha_0 = (1-2\upsilon)\beta,\ \beta = (3\lambda + 2\mu)\alpha_t,\ \lambda_s = \lambda + \frac{T_0 \beta^2}{\rho C_e},\ \upsilon_s = \frac{\lambda_s}{2(\lambda_s + \mu)},\ s$$

is the Laplace transform variable and $A_0^{\pm}$, $B_0^{\pm}$ and $C_0^{\pm}$ are source coefficients. Their values, for various types of sources, are given in Table 1. The bar over symbols represents Laplace transform with respect to *t*.

Table 1 Source coefficients for various sources in thermoelastic medium. The upper and lower signs are for $z > h$ and $z < h$ respectively.

Source	$A_0^{\pm}$	$B_0^{\pm}$	$C_0^{\pm}$	**Upper or lower solution**
Horizontal line force	$\frac{cc_1 k F_y}{2\pi(1-\upsilon)s^2 m}$	$\frac{-F_y\left(1-2\upsilon-c_1+\frac{2cc_1k^2}{s}\right)}{4\pi s(1-\upsilon)k^2}$	$\frac{(1+c_1)F_y}{4\pi(1-\upsilon)sk^2}$	Upper
Vertical line force	$\pm\frac{cc_1 F_z}{2\pi(1-\upsilon)s^2}$	$\pm\frac{F_z}{2\pi s}\left(\frac{1}{k^2}-\frac{cc_1}{s(1-\upsilon)}\right)$	$\pm\frac{(1+c_1)F_z}{4\pi(1-\upsilon)sk^2}$	Lower
Line heat source	$\frac{-(1-2\upsilon)\beta c q'}{2\pi m \lambda_0 (1-\upsilon) s^2}$	$\frac{(1-2\upsilon)\beta c q'}{2\pi k \lambda_0 (1-\upsilon) s^2}$	0	Lower

Double couple (yz) $+(zy)$ $\left(F_{yz}=F_{zy}=D_{yz}\right)$	$\pm\dfrac{c_1ckD_{yz}}{\pi(1-\upsilon)s^2}$	$\mp\dfrac{c_1ckD_{yz}}{\pi(1-\upsilon)s^2}$	$\pm\dfrac{(1+c_1)D_{yz}}{2\pi(1-\upsilon)sk}$	Upper
Double couple (zz) $-(yy)$ $(F_{yy}=F_{zz}=D'_{yz})$	$\dfrac{c_1c(m^2+k^2)D'_{yz}}{2\pi(1-\upsilon)ms^2}$	$-\dfrac{c_1ckD'_{yz}}{\pi(1-\upsilon)s^2}$	$\dfrac{(1+c_1)D'_{yz}}{2\pi(1-\upsilon)sk}$	Lower

F_y, F_z are magnitude of line forces, q' is the heat generated per unit length and $c_1=\dfrac{(\upsilon_s-\upsilon)}{(1-\upsilon_s)}$

3. Governing Equations and General Solutions

3.1 Solutions for poroelastic medium: The parameters that characterize an isotropic poroelastic medium are: Biot-Willis coefficient α, shear modulus μ', drained Poisson's ratio υ', hydraulic diffusivity c', Skempton's coefficient B, undrained Poisson's ratio υ_u and Darcy's permeability χ.

The Biot's stress function F is defined as

(3.1) $$\sigma'_{yy}=\frac{\partial^2F}{\partial z^2},\quad \sigma'_{zz}=\frac{\partial^2F}{\partial y^2},\quad \sigma'_{yz}=-\frac{\partial^2F}{\partial y\partial z}$$

and the governing equations of poroelastic medium[25] take the form

(3.2) $$\nabla^4F+2\eta'\nabla^2p=0,$$

(3.3) $$\left(\nabla^2-\frac{\partial}{c'\partial t}\right)\left(\nabla^2F+\frac{3p}{B(1+\upsilon_u)}\right)=0,$$

where $\nabla^2 \equiv \frac{\partial^2}{\partial y^2} + \frac{\partial^2}{\partial z^2}$, $\eta' = \frac{(1-2\upsilon')\alpha}{2(1-\upsilon')}$, σ'_{ij} are the stress components and p is the pore pressure.

Applying Laplace transform on Eqs. (3.2)-(3.3) and solving then, we get

$$\bar{F} = \int_0^\infty \Phi_1 \begin{pmatrix} \sin ky \\ \cos ky \end{pmatrix} dk, \tag{3.4}$$

$$\bar{p} = \int_0^\infty \Psi_1 \begin{pmatrix} \sin ky \\ \cos ky \end{pmatrix} dk, \tag{3.5}$$

where

$$\Phi_1 = \left(A_1 e^{m'z} + (B_1 + kzC_1)e^{kz} \right), \tag{3.6}$$

$$\Psi_1 = \zeta'\left(\frac{s}{\gamma' c'} A_1 e^{m'z} - k^2 C_1 e^{kz}\right), \tag{3.7}$$

$m' = \left(k^2 + \frac{s}{c'}\right)^{1/2}$, $\zeta' = \frac{2}{3}(1+\upsilon_u)B$, $\gamma' = \frac{2(\upsilon' - \upsilon_u)}{(1-\upsilon')}$ and A_1, B_1 and C_1 are arbitrary constants.

The corresponding stresses are obtained as

$$\bar{\sigma}'_{yy} = \int_0^\infty G_1 \begin{pmatrix} \sin ky \\ \cos ky \end{pmatrix} dk, \tag{3.8}$$

$$\sigma'_{zz} = \int_0^\infty N_1 \begin{pmatrix} \sin ky \\ \cos ky \end{pmatrix} dk, \tag{3.9}$$

$$\bar{\sigma}'_{yz} = \int_0^\infty S_1 \begin{pmatrix} -\cos ky \\ \sin ky \end{pmatrix} dk, \tag{3.10}$$

where

(3.11) $$G_1 = m'^2 A_1 e^{m'z} + k^2 (B_1 + (2+kz)C_1)e^{kz},$$

(3.12) $$N_1 = -k^2 \left(A_1 e^{m'z} + (B_1 + kzC_1)e^{kz} \right),$$

(3.13) $$S_1 = k\left(m'A_1 e^{m'z} + k\left(B_1 + (1+kz)C_1 \right) e^{kz} \right),$$

The corresponding displacement components are

(3.14) $$2\mu'\overline{u}'_y = \int_0^\infty V_1 \begin{pmatrix} -\cos ky \\ \sin ky \end{pmatrix} dk,$$

(3.15) $$2\mu'\overline{u}'_z = \int_0^\infty W_1 \begin{pmatrix} \sin ky \\ \cos ky \end{pmatrix} dk,$$

where

(3.16) $$V_1 = k\left(A_1 e^{m'z} + \{B_1 + (kz + 2 - 2\upsilon_u)C_1\}e^{kz} \right),$$

(3.17) $$W_1 = -\left(m'A_1 e^{m'z} + k(B_1 + (kz - 1 + 2\upsilon_u)C_1)e^{kz} \right),$$

The flux of fluid in z -direction is given by

(3.18) $$\overline{q}'_z = \int_0^\infty F_1 \begin{pmatrix} \sin ky \\ \cos ky \end{pmatrix} dk,$$

where

(3.19) $$F_1 = -\chi\zeta' \left(\frac{s}{\gamma'c'} m'A_1 e^{m'z} - k^3 C_1 e^{kz} \right).$$

3.2 Solutions for thermoelastic medium: For the thermoelastic medium, the Airy's stress function U is defined[33] as

(3.20) $$\sigma_{yy} = \frac{\partial^2 U}{\partial z^2},\ \sigma_{yz} = -\frac{\partial^2 U}{\partial y \partial z},\ \sigma_{zz} = \frac{\partial^2 U}{\partial y^2}$$

and the governing equations take the form

(3.21) $$\nabla^4 U + 2\eta \nabla^2 \theta = 0,$$

$$\lambda_0\nabla^2\theta-\left(\rho C_e+\frac{\alpha_0{}^2T_0}{\mu(1-2\upsilon)}\right)\dot{\theta}-\frac{\alpha_0T_0}{2\mu}(\nabla^2\dot{U})=0, \tag{3.22}$$

where σ_{ij} are stresses in thermoelastic medium, θ is the temperature difference function and $\eta=\dfrac{\alpha_0}{2(1-\upsilon)}$.

Application of Laplace transform on Eqs. (3.21)-(3.22) and simplification thereafter results into

$$(\nabla^2-\frac{s}{c})\nabla^2\bar{\theta}=0, \tag{3.23}$$

$$(\nabla^2-\frac{s}{c})\nabla^4\bar{U}=0. \tag{3.24}$$

After taking into consideration the line source which is acting in the thermoelastic half-space, the general solutions of Eqs. (3.23)-(3.24) become

$$\bar{U}=\bar{U}_0+\int_0^\infty \Phi_2\begin{pmatrix}\sin ky\\ \cos ky\end{pmatrix}dk, \tag{3.25}$$

$$\bar{\theta}=\bar{\theta}_0+\int_0^\infty \Psi_2\begin{pmatrix}\sin ky\\ \cos ky\end{pmatrix}dk, \tag{3.26}$$

Where

$$\Phi_2=A_2e^{-mz}+(B_2+kzC_2)e^{-kz}, \tag{3.27}$$

$$\Psi_2=\zeta(\frac{s}{\gamma c}A_2e^{-mz}+k^2C_2e^{-kz}), \tag{3.28}$$

A_2, B_2 and C_2 may be functions of k. $\bar{U}_0$ and $\bar{\theta}_0$ are given in Eqs. (2.2) and (2.3). Eq. (3.20) gives

$$\bar{\sigma}_{yy}=\int_0^\infty G_2\begin{pmatrix}\sin ky\\ \cos ky\end{pmatrix}dk, \tag{3.29}$$

$$\bar{\sigma}_{yz} = \int_0^\infty S_2 \begin{pmatrix} \cos ky \\ -\sin ky \end{pmatrix} dk, \tag{3.30}$$

$$\bar{\sigma}_{zz} = \int_0^\infty N_2 \begin{pmatrix} \sin ky \\ \cos ky \end{pmatrix} dk, \tag{3.31}$$

where

$$\begin{aligned} G_2 &= m^2 A_0 e^{-m|z-h|} + k^2 (B_0 - 2C_0 + k|z-h| C_0) e^{-k|z-h|} \\ &\quad + m^2 A_2 e^{-mz} + k^2 (B_2 - (2-kz)C_2) e^{-kz}, \end{aligned} \tag{3.32}$$

$$\begin{aligned} S_2 &= k[\pm(mA_0 e^{-m|z-h|} + k(B_0 - (1-k|z-h|)C_0) e^{-k|z-h|}) \\ &\quad + mA_2 e^{-mz} + k(B_2 - (1-kz)C_2) e^{-kz}], \end{aligned} \tag{3.33}$$

$$\begin{aligned} N_2 &= -k^2 [A_0 e^{-m|z-h|} + (B_0 + k|z-h| C_0) e^{-k|z-h|} \\ &\quad + A_2 e^{-mz} + (B_2 + kzC_2) e^{-kz}]. \end{aligned} \tag{3.34}$$

The components of displacement can be expressed as

$$2\mu \bar{u}_y = \int_0^\infty V_2 \begin{pmatrix} -\cos ky \\ \sin ky \end{pmatrix} dk, \tag{3.35}$$

$$2\mu \bar{u}_z = \int_0^\infty W_2 \begin{pmatrix} \sin ky \\ \cos ky \end{pmatrix} dk, \tag{3.36}$$

where

$$\begin{aligned} V_2 &= k\Big[A_0 e^{-m|z-h|} + (B_0 + (k|z-h| + 2\upsilon_s - 2)C_0) e^{-k|z-h|} \\ &\quad + A_2 e^{-mz} + (B_2 + (kz + 2\upsilon_s - 2)C_2) e^{-kz} \Big], \end{aligned} \tag{3.37}$$

$$\begin{aligned} W_2 &= \pm(mA_0 e^{-m|z-h|} + k(B_0 + (1 - 2\upsilon_s + k|z-h|)C_0) e^{-k|z-h|}) \\ &\quad + mA_2 e^{-mz} + (B_2 + k(1 - 2\upsilon_s + kz)C_2) e^{-kz}. \end{aligned} \tag{3.38}$$

The heat flux in z -direction is obtained as

$$\bar{q}_z = -\lambda_0 \bar{\theta},_z = \int_0^\infty F_2 \begin{pmatrix} \sin ky \\ \cos ky \end{pmatrix} dk, \tag{3.39}$$

where

$$F_2 = \lambda_0 \zeta \left[\pm \left(\frac{s}{\gamma c} m A_0 e^{-m|z-h|} + k^3 C_0 e^{-k|z-h|} \right) + \frac{s}{\gamma c} m A_2 e^{-mz} + k^3 C_2 e^{-kz} \right]. \tag{3.40}$$

4. Boundary Conditions

At the interface of half-spaces, the displacements and stresses are continuous. Hence

$$u'_y = u_y, \quad u'_z = u_z, \quad \sigma'_{yz} = \sigma_{yz}, \quad \sigma'_{zz} = \sigma_{zz} \text{ at } z = 0. \tag{4.1}$$

Also, the interface is supposed to be adiabatic and impermeable. Hence

$$q_z = 0 \text{ and } q'_z = 0 \text{ at } z = 0. \tag{4.2}$$

Let A_0^- (A_0^+), B_0^- (B_0^+) and C_0^- (C_0^+) be the values of A_0, B_0 and C_0 for $z < h$ ($z > h$) respectively. The boundary conditions (4.1) and (4.2) yield the system

$$\begin{cases} mA_2 + kB_2 - kC_2 + m'A_1 + kB_1 + kC_1 = mA_0^- e^{-mh} + (B_0^- + C_0^- kh - C_0^-) ke^{-kh}, \\ A_2 + B_2 - A_1 - B_1 = -A_0^- e^{-mh} - (B_0^- + C_0^- kh) e^{-kh}, \\ A_2 + B_2 + 2(\upsilon_s - 1)C_2 - \mu_r A_1 - \mu_r B_1 - 2\mu_r (1-\upsilon_u) C_1 \\ \qquad = -A_0^- e^{-mh} - (B_0^- + C_0^- (2\upsilon_s - 2 + kh)) e^{-kh}, \\ mA_2 + kB_2 + k(1-2\upsilon_s)C_2 + m'\mu_r A_1 + \mu_r kB_1 - \mu_r k(1-2\upsilon_u)C_1 \\ \qquad = mA_0^- e^{-mh} + (B_0^- + C_0^- (1-2\upsilon_s + kh) ke^{-kh}, \\ \dfrac{ms}{\gamma c} A_2 + k^3 C_2 = \dfrac{ms}{\gamma c} A_0^- e^{-mh} + k^3 C_0^- e^{-kz}, \\ \dfrac{m's}{\gamma' c'} A_1 - k^3 C_1 = 0, \end{cases} \tag{4.3}$$

where $\mu_r = \mu / \mu'$.

When these conditions are enforced, the unknowns are determined as:

$$(4.4)\quad \begin{cases} A_1 = -\dfrac{Q_2\Omega_1 k}{m'-k} C_0^- e^{-kh},\ C_1 = -Q_2 C_0^- e^{-kh}, \\ B_1 = Q_1\left(A_0^- e^{-mh} + \left(B_0^- + C_0^- kh\right)e^{-kh}\right) + \dfrac{1}{2}\left(-Q_1\left(1+\Omega_2\right) + Q_2\left(1+\Omega_1 + \dfrac{2k\Omega_1}{m'-k}\right)\right)C_0^- e^{-kh}, \\ A_2 = A_0^- e^{-mh} + \dfrac{2(1-Q_1)\Omega_2 k}{(m-k)(1+\Omega_2)}\left(A_0^- e^{-mh} + \left(B_0^- + C_0^- kh\right)e^{-kh}\right) + \dfrac{Q_1\Omega_2 k}{m-k} C_0^- e^{-kh}, \\ B_2 = -A_0^- e^{-mh} + (Q_1 - 1)\left(1 - \dfrac{2\Omega_2 k}{(k-m)(1+\Omega_2)}\right)\left(A_0^- e^{-mh} + \left(B_0^- + C_0^- kh\right)e^{-kh}\right) \\ \qquad + \dfrac{1}{2}\left(-Q_1\left(1+\Omega_2\right) + Q_2\left(1+\Omega_1\right) - \dfrac{2Q_1\Omega_2 k}{m-k}\right)C_0^- e^{-kh}, \\ C_2 = \dfrac{2\left(Q_1 - 1\right)}{\left(1+\Omega_2\right)}\left(A_0^- e^{-mh} + \left(B_0^- + C_0^- kh\right)e^{-kh}\right) - \left(Q_1 - 1\right)C_0^- e^{-kh}, \end{cases}$$

where,

$$P_1 = \frac{4\upsilon_s - 3 - \mu_r}{1-\mu_r}, \quad P_2 = \frac{\left(4\upsilon_u - 3\right)\mu_r - 1}{1-\mu_r}, \quad Q_1 = \frac{P_1 - 1}{(P_1 + \Omega_2)}, \quad Q_2 = \frac{\left(P_1 - 1\right)}{(P_2 - \Omega_1)},$$

$$\Omega_1 = \frac{k^2\gamma'}{m'(m'+k)},\ \Omega_2 = \frac{k^2\gamma}{m(m+k)}.$$

Using these values of A_1, A_2, B_1, B_2, C_1 and C_2 in Eqs. (3.5)-(3.19), (3.26)-(3.40), the integral expressions are obtained for the displacement and stress components in both the half-spaces, pore pressure and fluid flux in poroelastic half-space and the temperature difference function and heat flux in thermoelastic half-space in terms of the source coefficients A_0^-, B_0^- and C_0^-. Numerical computation of these integrals is possible for every value of t. But, their exact expressions can be obtained for two special limiting cases:

(i) $t \to 0$ i.e. there is no time for net flow of heat (fluid flow) in thermoelastic (poroelastic) medium which correspond to the adiabatic (undrained) conditions;

(ii) $t \to \infty$ i.e. sufficient time for flow of heat (fluid flow), which implies the isothermal (drained) conditions.

5. Vertical Dip-Slip Fault: Particular Solutions

The double couple $(yz)+(zy)$, having moment $D_{yz}=\mu b\,dl$, corresponds to a vertical dip-slip fault[34]. Here b is the slip and dl is the width of the dislocation.

The source coefficients for the dip-slip fault (Table 1) are

$$A_0^- = -\frac{cc_1kD_{yz}}{\pi(1-\upsilon)s^2},\ B_0^- = \frac{cc_1kD_{yz}}{\pi(1-\upsilon)s^2}, C_0^- = -\frac{D_{yz}(1+c_1)}{2\pi ks(1-\upsilon)} \tag{5.1}$$

and the upper solution is to be selected in the integrals.

5.1 Poroelastic half-space: Biot's stress function, stresses, displacements and pore pressure are obtained for the following particular cases:

Case (i) Undrained condition;

$$F = \frac{-D_{yz}}{2\pi(1-\upsilon_s)}\left[-\frac{1}{2}(Q_3+Q_4)\tan^{-1}\left(\frac{y}{h-z}\right)+(Q_3h+Q_4z)\frac{y}{R_1^2}\right], \tag{5.2}$$

$$\sigma'_{yy} = -\frac{D_{yz}}{2\pi(1-\upsilon_s)}\frac{y}{R_1^4}\begin{bmatrix} Q_3(z-3h)+Q_4(3h-5z) \\ +8(Q_4z+Q_3h)\dfrac{(h-z)^2}{R_1^2}\end{bmatrix}, \tag{5.3}$$

$$\sigma'_{yz} = \frac{-D_{yz}}{2\pi(1-\upsilon_s)}\left[\frac{(Q_4-Q_3)}{2R_1^2}+\frac{\big(Q_3(z-7h)+Q_4(h-7z)\big)(z-h)}{R_1^4}+\frac{8(Q_4z+Q_3h)(z-h)^3}{R_1^6}\right], \tag{5.4}$$

$$\sigma'_{zz} = -\frac{D_{yz}}{2\pi(1-\upsilon_s)}\frac{y}{R_1^4}\begin{bmatrix} Q_3(3h-z)+Q_4(z+h)-8(Q_3h \\ +Q_4z)\dfrac{(h-z)^2}{R_1^2}\end{bmatrix}, \tag{5.5}$$

$$u'_y = -\frac{D_{yz}}{4\pi\mu'(1-\upsilon_s)}\frac{1}{R_1^2}\times$$

(5.6)
$$\left[\frac{1}{2}[Q_3(3h-z)+Q_4(h+z+4(1-\upsilon_u)(z-h)]\right.$$
$$\left.-2(Q_4 z+Q_3 h)\frac{(h-z)^2}{R_1^2}\right],$$

(5.7)
$$u'_z = -\frac{D_{yz}}{4\pi\mu'(1-\upsilon_s)}\frac{y}{R_1^2}\begin{bmatrix}\frac{1}{2}\left(Q_3-Q_4+4(1-\upsilon_u)Q_4\right) \\ -2(Q_4 z+Q_3 h)\frac{(h-z)}{R_1^2}\end{bmatrix}$$

(5.8)
$$p = \frac{D_{yz}\zeta' y}{\pi(1-\upsilon_s)}\left(Q_4\frac{(h-z)}{R_1^4}\right),$$

where $R_1^2 = y^2+(z-h)^2$, $Q_3 = \left(P_1-1\right)/P_1$, $Q_4 = -\left(P_1-1\right)/P_2$.

Case (ii) Drained condition;

We denote

(5.9) $$P_3 = \frac{4\upsilon-3-\mu_r}{1-\mu_r},\ P_4 = \frac{1-\mu_r}{1+3\mu_r-4\mu_r\upsilon'}\quad Q_5 = \frac{P_3-1}{P_3},\ Q_6 = P_4\left(P_3-1\right).$$

The expressions for displacement and stress components for the drained condition are similar to that for the undrained condition if we replace υ_u by υ', υ_s by υ, Q_3 by Q_5 and Q_4 by Q_6. The pore pressure is found zero.

5.2 Thermoelastic half-space: Airy stress function, stresses, displacements and temperature difference function are obtained for the following particular cases:

Case (i) Adiabatic condition;

(5.10)
$$U = \frac{D_{yz}}{2\pi(1-\upsilon_s)}\left[\frac{y\left(z-h\right)}{R_1^2}-\left\{Q_8\tan^{-1}\left(\frac{y}{z+h}\right)\right.\right.$$
$$\left.\left.-Q_7\frac{y(z-h)}{R_2^2}+4Q_7 h\frac{yz(h+z)}{R_2^4}\right\}\right],$$

$$\sigma_{yy}=\frac{D_{yz}y}{\pi(1-\upsilon_s)}\left[\left(-3+4\frac{(z-h)^2}{R_1^2}\right)\frac{(z-h)}{R_1^4}\right.$$
$$-\left\{\frac{Q_8(h+z)+Q_7(5h+3z)}{R_2^4}\right. \tag{5.11}$$
$$\left.\left.-4Q_7(h+z)(z^2+3h^2+10hz)\frac{1}{R_2^6}+48Q_7hz\frac{(h+z)^3}{R_2^8}\right\}\right],$$

$$\sigma_{zz}=\frac{D_{yz}y}{\pi(1-\upsilon_s)}\left[\frac{(z-h)}{R_1^4}\left(1-4\frac{(z-h)^2}{R_1^2}\right)\right.$$
$$\left.-\frac{1}{R_2^4}\left\{-Q_7(z-h)-Q_8(h+z)-\frac{48Q_7hz(h+z)^3}{R_2^4}+\frac{4Q_7(h+z)(z^2-h^2+6hz)}{R_2^2}\right\}\right], \tag{5.12}$$

$$\sigma_{yz}=\frac{D_{yz}}{2\pi(1-\upsilon_s)}\left[\frac{1}{R_1^2}\left(1-8\left(\frac{z-h}{R_1}\right)^2+8\left(\frac{z-h}{R_1}\right)^4\right)\right.$$
$$-\frac{1}{R_2^2}\left\{-Q_7-Q_8+\frac{(8Q_7+2Q_8)(h+z)^2+12Q_7hz}{R_2^2}\right. \tag{5.13}$$
$$\left.\left.-\frac{8Q_7(z+h)^2\left((z+h)^2+12hz\right)}{R_2^4}+96Q_7hz\frac{(h+z)^4}{R_2^6}\right\}\right],$$

$$u_y=\frac{D_{yz}}{4\pi\mu(1-\upsilon_s)}\left[\frac{(z-h)}{R_1^2}\left(3-2\upsilon_s-2\frac{(z-h)^2}{R_1^2}\right)\right.$$
$$-\frac{1}{R_2^2}\left\{-Q_8(h+z)-Q_7(z-h)-2Q_7(1-\upsilon_s)(z+3h)-16Q_7hz\frac{(h+z)^3}{R_2^4}\right. \tag{5.14}$$
$$\left.\left.+\frac{2Q_7\left((h+z)\left(z-h+4(1-\upsilon_s)h\right)+6hz\right)(h+z)}{R_2^2}\right\}\right],$$

(5.15)
$$u_z = \frac{D_{yz} y}{4\pi\mu(1-\upsilon_s)}\left[\frac{1}{R_1^2}\left((1-2\upsilon_s)+\frac{2(z-h)^2}{R_1^2}\right) - \frac{1}{R_2^2}\left\{Q_8 - Q_7(1-2\upsilon_s)+\frac{16Q_7 hz(z+h)^2}{R_2^4} - \frac{2Q_7\left(\left(z-h-2h(1-2\upsilon_s)\right)(h+z)+2hz\right)}{R_2^2}\right\}\right],$$

(5.16)
$$\theta = \frac{D_{yz}\zeta y}{\pi(1-\upsilon_s)}\left[\frac{(z-h)}{R_1^4}+Q_7\left(\frac{z+3h}{R_2^4}-\frac{8h(z+h)^2}{R_2^6}\right)\right],$$

where $R_2^2 = y^2+(z+h)^2$, $Q_7 = Q_3 - 1$, $Q_8 = -\frac{1}{2}(Q_3+Q_4)$.

Case (ii) Isothermal Case;
We denote

(5.17)
$$Q_9 = Q_5 - 1, Q_{10} = -\frac{1}{2}(Q_5+Q_6)$$

The expressions for displacement and stress components for the isothermal condition are similar to that for the adiabatic condition if we replace υ_s by υ, Q_3 by Q_5, Q_4 by Q_6, Q_7 by Q_9 and Q_8 by Q_{10}.

6. Numerical results and discussion

The stresses and displacements in the two half-spaces, temperature function in thermoelastic medium and pore pressure in porous medium due to a vertical dip-slip dislocation source through a point $(0,0,h)$ are given in Eqs. (5.3)-(5.8) and (5.11)-(5.16) for adiabatic and undrained conditions. For isothermal and drained conditions, the solutions can be obtained by replacing υ_u by υ', υ_s by υ, Q_3 by Q_5, Q_4 by Q_6, Q_7 by Q_9 and Q_8 by Q_{10} in Eqs. (5.3)-(5.7) and (5.11)-(5.15). The pore pressure and temperature function become zero in these cases.

6.1 Validation of the solutions: A comparison between the particular cases of the results obtained in this paper and those obtained in earlier studies is made to verify the present results.

It is observed that

(i) If the thermoelastic medium is made elastic by taking $\upsilon_s = \upsilon$ or $\beta = 0$, the results coincide with that of Rani and Singh[25].

(ii) By taking the rigidity of poroelastic half-space zero (the model will be a uniform thermoelastic half-space), the results coincide with that of Vashishth and Rani[33].

(iii) For the limiting case $t \to \infty$ (isothermal and drained conditions), the results coincide with that obtained by Singh et al.[3].

6.2 Numerical computation: For the numerical computation of the results, the parameters of thermoelastic and poroelastic solid half-spaces are taken as $\upsilon = 0.25$, $\upsilon_s = 0.3023$, $\alpha_t = 3.11\times10^{-5}K^{-1}$, $T_0 = 1000K$, $c = 5.2385\times10^{-7}m^2/s$, $B = 0.88$, $\alpha = 0.65$, $c' = 5.3\times10^{-3}m^2/s$, $\upsilon' = 0.12$ and $\upsilon_u = 0.31$. For the poroelastic half-space, the parameters are taken for Ruhr Sandstone[19]. The thermoelastic half-space is assumed Possionian and υ_s and c are calculated for the pyrope rich garnet[35]. The displacements, stresses, pore pressure and temperature difference functions are computed numerically for vertical dip-slip dislocation (Figs. 2 to 13) and line heat source (Figs. 14-15) and are presented graphically.

The non-dimensional quantities are defined as

$$T = \frac{2c't}{h^2}, Y = \frac{y}{h}, Z = \frac{z}{h}, U_i = \frac{hu_i}{bdl}, U_i' = \frac{hu_i'}{bdl},$$
$$\Sigma_{ij} = \frac{h^2\sigma_{ij}}{\mu bdl}, \Sigma_{ij}' = \frac{h^2\sigma_{ij}'}{\mu bdl}, P = \frac{h^2 p}{\mu bdl}, \Theta = \frac{h^2\alpha_t\theta}{bdl}. \tag{6.1}$$

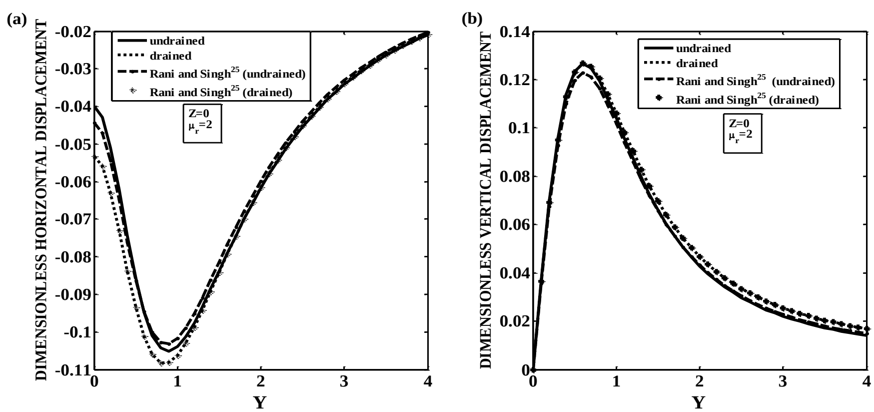

Figure 2. Variation of the displacements with Y at $Z = 0$ for $\mu_r = 2$: (a) horizontal displacement (b) vertical displacement.

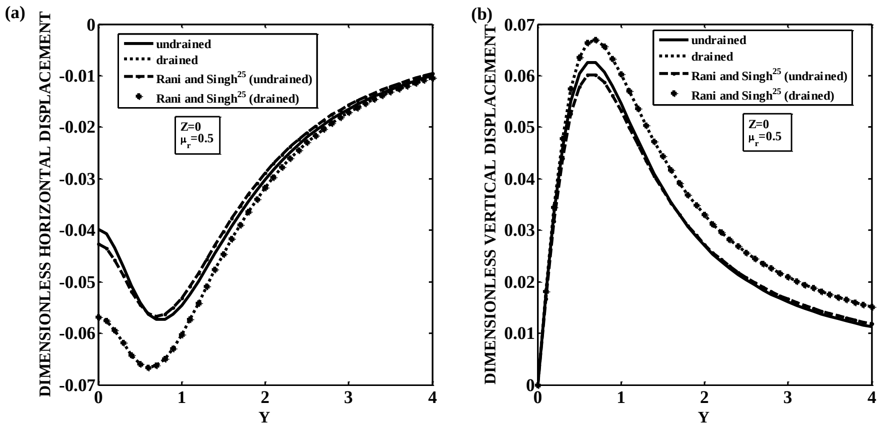

Figure 3. Variation of displacements with Y at Z =0 for $\mu_r = 1/2$: (a) horizontal displacement (b) vertical displacement.

Figures 2 and 3 depict the variation of displacements along the horizontal distance from the fault (Y) at the interface Z =0 for $\mu_r = 2$ and $\mu_r = 1/2$ respectively for undrained and drained conditions. It is observed that the difference between undrained and drained horizontal displacement is large near the fault line (Y =0) whereas for the vertical displacement, this difference is noticed as Y increases. The magnitude of the displacements is large for $\mu_r = 2$, i.e., when the rigidity of thermoelastic medium is greater than that of the poroelastic medium. The more stiff the poroelastic half-space is, the more difference in undrained and drained displacements is observed. The present results for drained conditions match with the corresponding results obtained by Rani and Singh[25]. However, for the undrained conditions, the difference due to inclusion of thermal effect in the half-space containing the source is explicitly observed.

As the expressions of displacements, stresses, temperature difference function and pore pressure are in Laplace transform domain, Schapery[36]'s formula for Laplace inversion is used to compute the results in time domain. The semi infinite integrals are evaluated by using Gauss quadrature formula. The variation of pore pressure with time T at Z =0, -1, -2 and Y =1 is demonstrated in Fig. 4. The pore pressure has highest amplitude at Z =0 for all times and diffuses with time at all depths. Fig. 5a and b depict the variation of pore pressure with Y at Z =0 and Z = -1 at different times T=0 , 0.1, 1, 10 , ∞. It is observed that the pore pressure is maximum in undrained state (T=0) and zero in drained state ($T \to \infty$) which is physically acceptable as there is sufficient time to diffuse the fluid from the medium.

The point of maxima moves away along Y as T increases. Depth profile of pore pressure is exhibited in Fig. 6 for T=0, 0.1, 1, 10, ∞. A sharp decay in pore pressure with depth is observed. The graphs for pore pressure in Figs. 4, 5 and 6 are same as that plotted by Rani and Singh[25]. It has been verified analytically for undrained case.

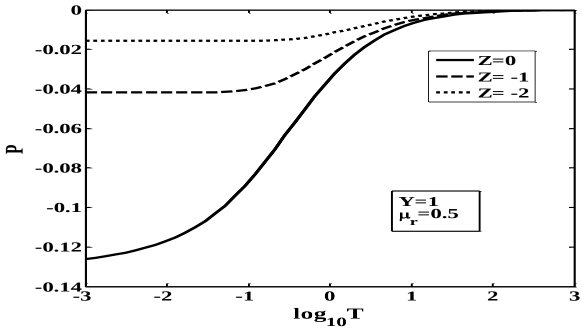

Figure 4. Variation of pore pressure against dimensionless time T for $\mu_r = 1/2$ at Z =0, -1, -2.

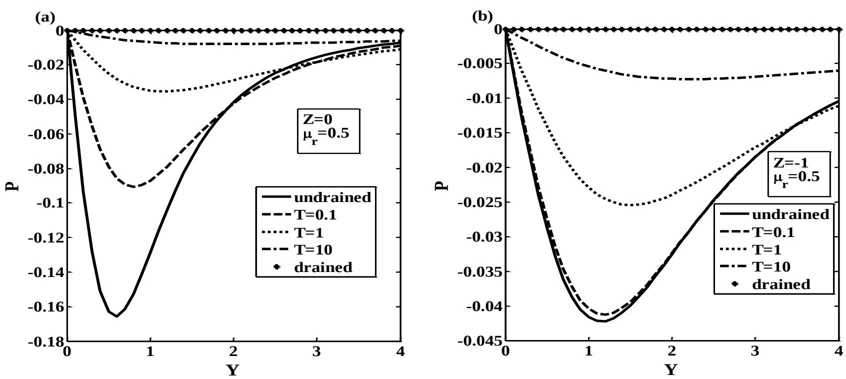

Figure 5. Pore pressure distribution with Y for $\mu_r = 1/2$ (a) Z =0, (b) Z = -1.

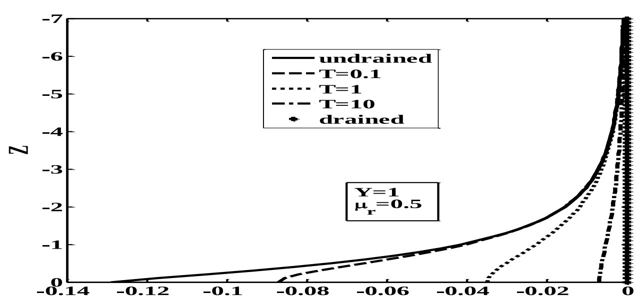

Figure 6. Variation of pore pressure with depth for $\mu_r = 1/2$ at Y =1.

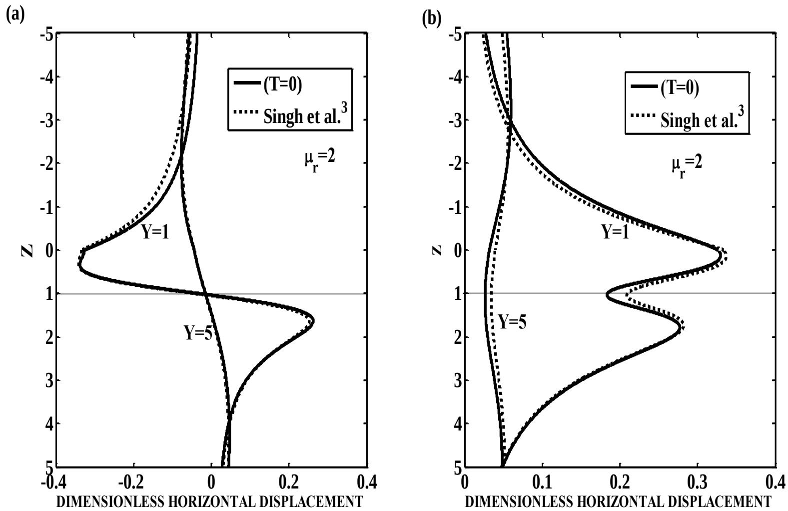

Figure 7. Variation of horizontal displacements (a) and vertical displacement (b) with Z at Y =1, 5 for $\mu_r = 2$. (Here the scale factor π is used)

Depth profiles of the displacements, for the two limiting cases $T \to 0$ and $T \to \infty$, at Y =1, 5 for $\mu_r = 2$ are plotted in Fig. 7 and for $\mu_r = 2/3$, in Fig. 8. The time $T \to 0$, in thermoelastic medium corresponds to adiabatic condition and undrainded condition in poroelastic medium and $T \to \infty$ corresponds to isothermal and drained conditions respectively. For $T \to \infty$, the graphs of displacements coincide with that of Singh et al.[3]. Figures 9 and 10 depict variation of displacements along Y at four receivers Z =-0.5, 0, 0.5 ,5 for $\mu_r = 2$ and $\mu_r = 2/3$ respectively. The displacements for two limiting cases are compared.

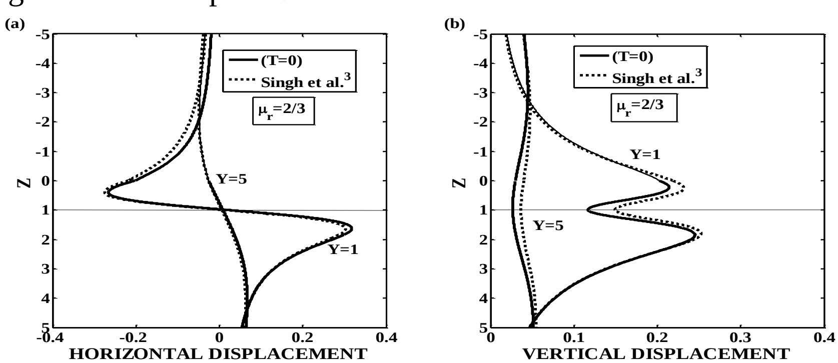

Figure 8. Variation of horizontal displacements (a) and vertical displacement (b) with Z for Y =1,5 and $\mu_r = 2/3$.

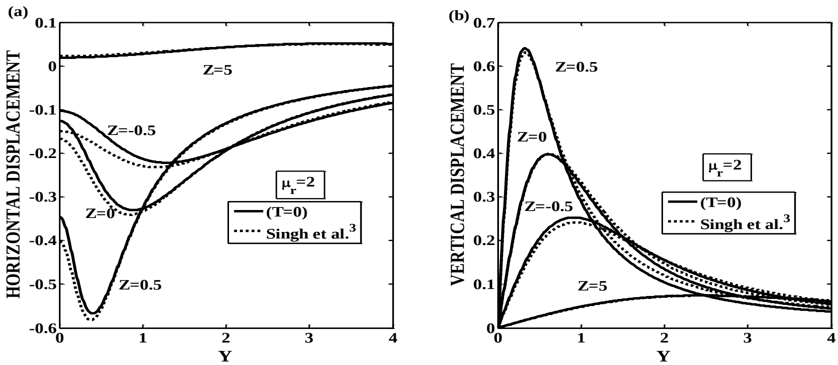

Figure 9. Variation of displacements with Y at Z =-0.5, 0, 0.5, 5 for $\mu_r = 2$: (a) horizontal, (b) vertical displacement

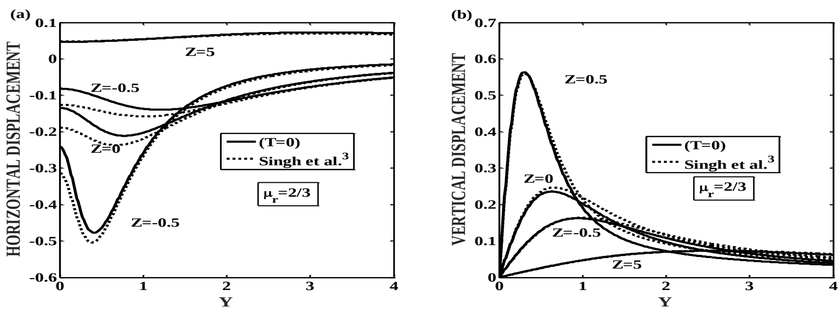

Figure 10. Variation of displacements with Y at Z =-0.5, 0, 0.5 ,5 for $\mu_r = 2/3$: (a) horizontal, (b) vertical displacement.

The variation of temperature increment function along dimensionless time T is demonstrated in Fig. 11 for $\mu_r = 2$ and Y =1, 2 at Z =0, 0.5, 1, 1.5, 2. The temperature difference function is negative between the interface and the fault line and positive below the fault line at all times. It is almost zero on the fault/ source line. Figure 11a shows that for Y =1, it attains its maximum and minimum values at Z =1.5 and Z =0.5 respectively. The point of maxima and minima shifted away to Z =2 and Z =0 for Y =2 as shown in Fig.11b.

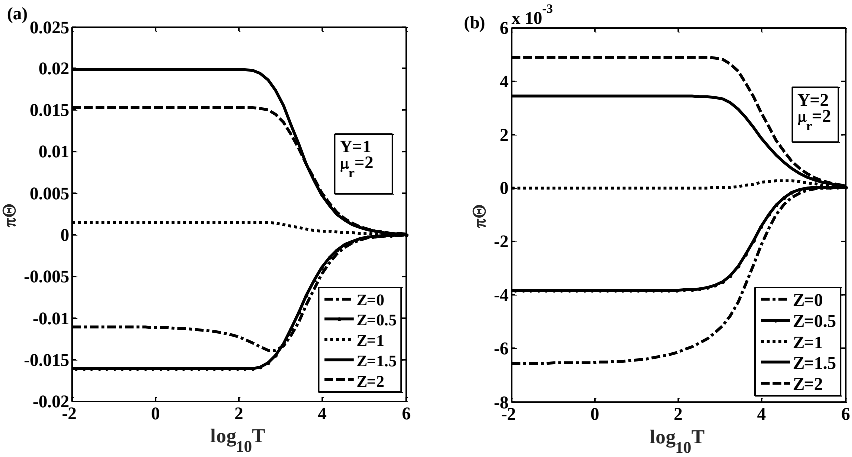

Figure 11. Variation of temperature function with T for $\mu_r = 2$ at Z =0, 0.5, 1, 1.5, 2: (a) Y =1, (b) Y =2.

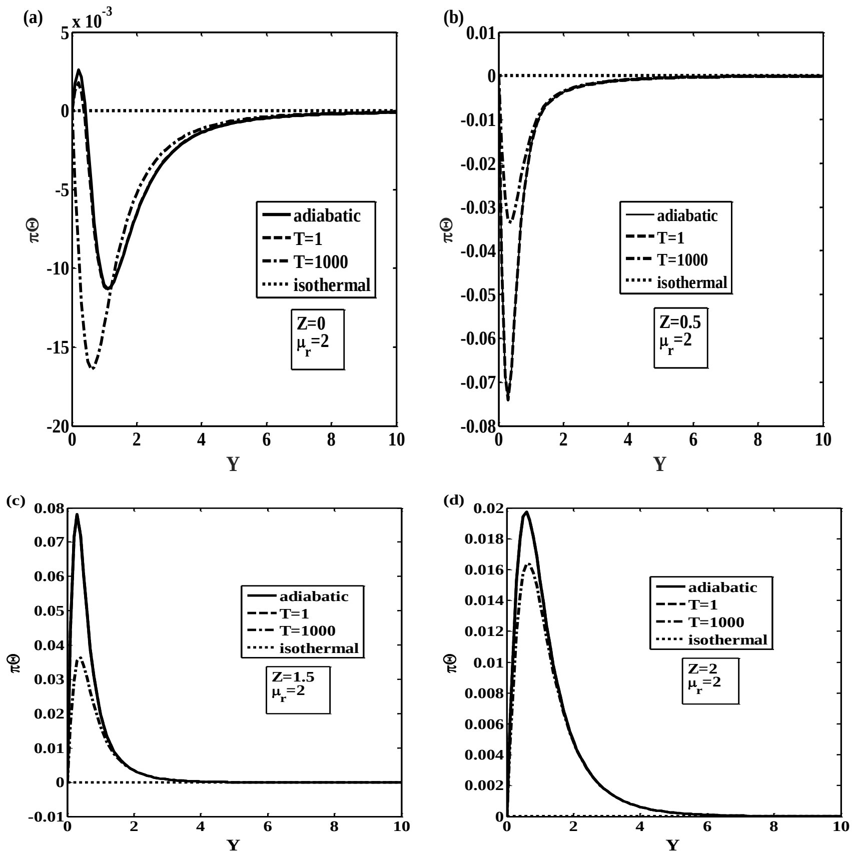

Figure 12. Variation of temperature function with Y for $\mu_r = 2$: (a) Z =0, (b) Z =0.5, (c) Z =1.5, (d) Z =2.

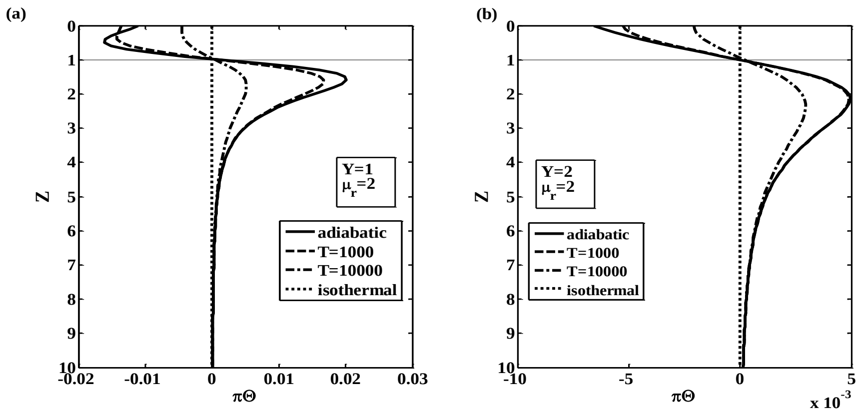

Figure 13. Variation of temperature function with Z for $\mu_r = 2$: (a) Y =1, (b) Y =2.

Figs. 12a to d present the variation of temperature difference along Y at Z =0, 0.5. 1.5, 2 respectively for T=0 (adiabatic), 1, 1000, ∞ (isothermal). It verifies the description of Fig. 11. It is noticed that at Z =0, temperature has maximum magnitude at T=1000, but in all other cases, maximum magnitude is observed for adiabatic condition. For isothermal condition, $\Theta = 0$. Depth profile of Θ is shown in Fig. 13 for Y =1 and 2. The temperature difference is noticeable 0< Z <4 and approaches to zero as Z increases.

For line heat source, the dimensionless quantities are defined as

$$Y = \frac{y}{h},\ Z = \frac{z}{h},\ U_i = \frac{\lambda_0 u_i}{q'\alpha_t},\ \Sigma_{ij} = \frac{\lambda_0 h \sigma_{ij}}{q'\mu\alpha_t},\ \Theta = \frac{\lambda_0 \theta h}{q'} \tag{6.2}$$

where q' is the amount of heat generated per unit length.

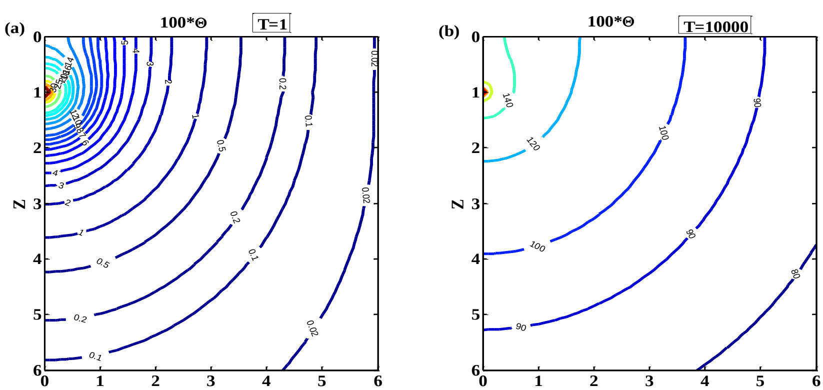

Figure 14. Variation of temperature function in thermoelastic medium due to heat source.

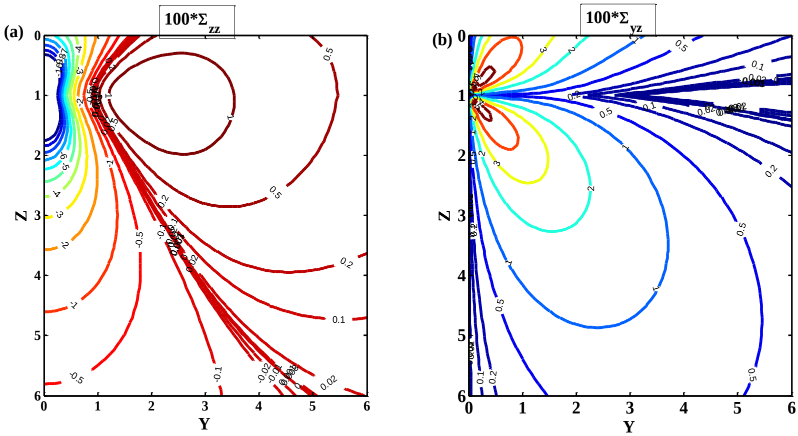

Figure 15. Distribution of stresses in thermoelastic medium due to heat source

Variation of temperature function due to line heat source is shown in Fig. 14. As the time increases, temperature increases. But as the distance from the heat source increases, the temperature function decreases. Contours for stresses in thermoelastic medium due to heat source are plotted in Fig. 15. These maps exhibit the variation of elastic field around the heat source.

7. Conclusion

A study of 2D quasi static deformation of a medium, composed of a homogeneous isotropic thermoelastic solid in welded contact with a homogeneous isotropic poroelastic solid due to a line source (horizontal and vertical line forces, dip-slip dislocation, heat source) in thermoelastic medium, is carried out. The solutions for dip-slip line dislocation are evaluated analytically for two limiting cases: adiabatic and isothermal conditions in thermoelastic medium and undrained and drained conditions in poroelastic medium. It is observed that the difference between undrained and drained horizontal displacement in poroelastic medium is large near the dip-slip fault line whereas for the vertical displacement, this difference is noticeable as distance from the fault increases. The amplitude of the displacements is large when the thermoelastic solid is stiffer than the poroelastic solid. The more rigid the poroelastic medium is, the more difference in drained and undrained displacements is observed. The pore pressure has maximum amplitude at interface for all times and diffuses with time at all depths. Between the interface and the fault line, the temperature decreases but it increases below the fault line. The maximum temperature difference has been observed for adiabatic condition. Contours for stresses in thermoelastic medium due to heat source exhibit the variation of elastic field around the heat source. So, it can be concluded that the effect of inclusion of thermoelasticity in the half-space containing the source is considerably different in comparison to elastic and/or poroelastic half-spaces.

References

1. R. S. Wu and Y. T. Chou, Line Force in a Two-Phase Orthotropic Medium, *Journal of Applied Mechanics,* **49** (1982), 55-61.

2. T. H. Heaton and R. E. Heaton, Static Deformations From Point Forces and Force Couples Located in Welded Elastic Poissonian Half-Spaces: Implications for Seismic Moment Tensors, *Bulletin of the Seismological Society of America*, **79** (1989), 813-841.

3. S. J. Singh, S. Rani and N. R. Garg, Displacements and Stresses in Two Welded Half-Spaces Caused by Two-Dimensional Sources, *Physics of the Earth and Planetary Interiors,* **70** (1992), 90-101

4. S. J. Singh and S. Rani, Static Deformation Due to Two-Dimensional Seismic Sources Embedded in an Isotropic is Half-Space in Welded Contact with an Orthotropic Half-Space, *Journal of Physics of the Earth*, **39** (1991), 599-618.

5. G. Kumari, S. J. Singh and K. Singh, Static Deformation of Two Welded Elastic Half-Spaces Caused by A Point Dislocation Source, *Physics of the Earth and Planetary Interiors,* **73** (1992), 53-76.

6. S. J. Singh and S. Rani, 2-D Modeling of the Crustal Deformation Associated with Strike-Slip and Dip-Slip Faulting in the Earth, *Proc. Indian Acad. Sci. (Earth Planet. Sci.),* **66** (1996), 187-215.

7. S. Rani and S. J. Singh, Static Deformation of Two Welded Half-Spaces Due to Dip-Slip Faulting, *Proceedings of the Indian Academy of Sciences-Earth and Planetary Sciences*, **101** (1992), 269-282.

8. S. J. Singh, G. Kumari and K. Singh, Static Deformation of Two Welded Elastic Half-Spaces Caused by a Finite Rectangular Fault, *Physics of the Earth and Planetary Interiors,* **79** (1993), 313-333

9. A. Kumar, S. Singh and J. Singh, Static Deformation of Two Welded Monoclinic Elastic Half-Spaces Due to a Long Inclined Strike-Slip Fault, *Proceedings of the Indian Academy of Sciences-Earth and Planetary Sciences,* **111** (2002), 125-131.

10. A. Kumar, S.J. Singh and J. Singh, Deformation of Two Welded Elastic Half-Spaces Due to a Long Inclined Tensile Fault, *Journal of Earth System Science,* **114** (2005), 97-103.

11. S. Rani and N. Bala, 2-D Deformation of Two Welded Half-Spaces Due to a Blind Dip-Slip Fault, *Journal of Earth System Science,* **115** (2006), 277-287.

12. S. Rani, N. Bala and R. C. Verma, Displacement Field Due to Nonuniform Slip Along a Long Dip-Slip Fault in Two Welded Half-Spaces, *Journal of Earth Science,* **23** (2012), 864-872.

13. M. Malik, M. Singh and J. Singh, Static Deformation Due to Long Tensile Fault Embedded in an Isotropic Half-Space in Welded Contact with an Orthotropic Half-Space, *International Journal of Scientific and Research Publications,* **2(11)** (2012), 1-12.

14. Y. Godara, R. K. Sahrawat and M. Singh, Static Deformation Due to a Long Tensile Fault of Finite Width in an Isotropic Half-Space Welded with an Orthotropic Half-Space, *Bulletin of Mathematical Sciences and Applications,* **3** (2014), 13-33.

15. Y. Godara, R. K. Sahrawat and M. Singh, Static Deformation Due to Two-Dimensional Seismic Sources Embedded in an Isotropic Half-Space in Smooth Contact with an Orthotropic Half-Space, *Global Journal of Mathematical Analysis,* **2** (2014), 169-183.

16. A. K. Vashisth, K. Rani and K. Singh, Quasi-Static Planar Deformation in a Medium Composed of Elastic and Thermoelastic Solid Half Spaces Due to Seismic Sources in an Elastic Solid, *Acta Geophysica*, **63** (2015), 605-633.

17. M. A. Biot, General Theory of Three-Dimensional Consolidation, *Journal of Applied Physics,* **12** (1941), 155-164.

18. M. A. Biot, General Solutions of The Equations of Elasticity and Consolidation for a Porous Material, *J. appl. Mech.,* **23** (1956), 91-96.

19. H. F. Wang, *Theory of Linear Poroelasticity*, Princeton University Press Princeton, NJ, 2000.

20. J. R. Rice, M. P. Cleary, Some Basic Stress Diffusion Solutions for Fluid-Saturated Elastic Porous Media with Compressible Constituents, *Reviews of Geophysics,* **14** (1976), 227-241.

21. H. F. Wang, Quasi-Static Poroelastic Parameters in Rock and Their Geophysical Applications, *Pure and Applied Geophysics,* **141**(1993), 269-286.

22. J. W. Rudnicki, Fluid Mass Sources and Point Forces in Linear Elastic Diffusive Solids, *Mechanics of Materials,* **5** (1986), 383-393.

23. E. Pan Dislocations In An Infinite Poroelastic Medium, *Acta Mechanica,* **87** (1991), 105-115.

24. I. Taguchi and M. Kurashige, Fundamental Solutions for a Fluid-Saturated, Transversely Isotropic, Poroelastic Solid, *International Journal for Numerical and Analytical Methods in Geomechanics,* **26** (2002), 299-321.

25. S. Rani and S. J. Singh, Quasi-Static Deformation Due to Two-Dimensional Seismic Sources Embedded in an Elastic Half-Space in Welded Contact with a Poroelastic Half-Space, *Journal of Earth System Science,* **116** (2007), 99-111.

26. R. Kumar, S. Rani and S. J. Singh, Quasi-Static Deformation Caused by a Long Tensile Dislocation in an Elastic Half-Space in Welded Contact with a Poroelastic Half-Space, *Journal of Porous Media*, **15** (2012), 283-291.

27. A. Kumar, K. Singh, and M. K. Sharma, Displacement and Stress Fields in a Poroelastic Half-Space Due to a Concentrated Force, *International Journal of Engineering Science and Technology (IJEST)*, **4** (2012), 2475-2484.

28. N. Kumari and A. Miglani, Plane Strain Deformation of a Poroelastic Half-Space in Welded Contact with Transversely Isotropic Elastic Half-Space. *International Journal of Engineering Science and Technology (IJEST)*, **4** (2012), 4555-4570.

29. N. Kumari and A. Miglani, Plane Strain Deformation of a Poroelastic Half-Space in Welded Contact with an Isotropic Elastic Half Space, *International Journal of Science and Technology*, **2** (2013), 44-59.

30. A. Miglani and N. Kumari, Plane Strain Deformation of a Poroelastic Half-Space Lying Over Another Poroelastic Half-Space, *Journal of Solid Mechanics*, **5** (2013), 418-435.

31. R. Verma, S. Rani, S. Singh, Deformation of a Poroelastic Layer Overlying an Elastic Half-Space Due to Dip-Slip Faulting, *International Journal for Numerical and Analytical Methods in Geomechanics*, **40** (2016), 391-405.

32. L. H. Pan, P. F. Hou and J. Y. Chen, 2D Steady-State General Solution and Fundamental Solution for Fluid-Saturated, Orthotropic, Poroelastic Materials, *Z. Angew. Math. Phys.*, **67** (2016), 84 (1-13).

33. A. K. Vashishth and K. Rani, Quasi-Static Deformation of a Uniform Thermoelastic Half-Space Due to Seismic Sources and Heat Source, *Journal of Solid Mechanics*, **10** (2018), 702-718.

34. T. Maruyama, On Two-Dimensional Elastic Dislocations in an Infinite and Semi-Infinite Medium, *Bulletin of the Earthquake Research Institute*, **44** (1966), 811–871.

35. T. J. Ahrens, *Mineral Physics and Crystallography: A Handbook of Physical Constants*, American Geophysical Union, 1995.

36. R. A. Schapery, Approximate Methods of Transform Inversion for Viscoelastic Stress Analysis, *Proc. 4th US Nat. Congr. Appl. Mech*., **2** (1962), 1075-1085.